January 2026
Volume 2
Issue 1

DOI: 10.48308/ijce.2026.107088

Comparative Assessment of CMR in Steel Seismic Force-Resisting Systems: A FEMA P-695 Statistical Analysis

Authors:

Parsa Rashvand[1], Pouya H. Khosravi[1], Mohammadjavad Hamidia[*, 1], Nemat Hassani[1]

Abstract

Evaluating the seismic collapse performance of steel structural systems is one of the primary objectives of the FEMA P-695 guideline. In this guideline, the collapse margin ratio (CMR) is defined as a quantitative measure of collapse capacity. Despite extensive research on the seismic performance of steel structural systems, a systematic statistical comparison among special moment-resisting frames (SMFs), special concentrically braced frames (SCBFs), and eccentrically braced frames (EBFs) has not yet been reported within the FEMA P-695 framework. To address this gap, 108 steel archetypes corresponding to a common seismic hazard level (S_{MT} = 0.5g) are selected and evaluated. The collapse margin ratio (CMR) values are statistically examined using descriptive and inferential statistical methods to identify significant differences in collapse performance among the three structural systems. Using one-way analysis of variance (ANOVA) and Tukey's post-hoc test, the differences in mean CMR among the three systems are examined. Results indicated that the effect of structural system type on CMR is statistically significant ($F = 8.19$, $p < 0.001$, $\eta^2 = 0.135$). The mean CMR values for SMF, SCBF, and EBF are found to be 2.34, 2.06, and 1.79, respectively. Tukey's test revealed that only the difference between SMF and EBF is significant at the 95% confidence level, while SCBF exhibits an intermediate performance. These findings underscore the importance of selecting an appropriate structural system during the preliminary design phase and can serve as a quantitative basis for revising Iran's seismic design provisions.

Keywords: FEMA P-695, Collapse Margin Ratio, Steel Moment-Resisting Frame, Concentrically Braced Frame, Eccentrically Braced Frame, Analysis of Variance

1. Faculty of Civil, Water and Environmental Engineering, Shahid Beheshti University, Tehran, Iran

*Corresponding Author: m_hamidia@sbu.ac.ir

1. Introduction

Destructive earthquakes in recent decades have demonstrated that structural collapse is the primary cause of human casualties and economic losses due to seismic events (Coburn & Spence, 2002; Spence & Coburn, 2006; Spence et al., 2007; Liel et al., 2011). Therefore, quantitative assessment of structural collapse capacity and understanding the factors influencing it are among the most important objectives of modern earthquake engineering (Liel et al., 2011). In this regard, the FEMA P-695 methodology provides a coherent framework for evaluating the seismic performance of structural systems and determining seismic design coefficients (Federal Emergency Management Agency, 2009).

This guideline, employing incremental dynamic analysis (IDA) and probabilistic methods, introduces the collapse margin ratio (CMR) as a quantitative measure of collapse capacity—an index that states the ratio of the median collapse spectral acceleration (S_{CT}) to the design spectral acceleration (S_{MT}) (Federal Emergency Management Agency, 2009). Steel lateral load-resisting systems, owing to their high ductility and favorable nonlinear behavior, are among the most widely used systems in mid-rise and high-rise buildings in seismically active regions (American Society of Civil Engineers, 2022; Road, Housing and Urban Development Research Center, 2026). Among these systems, special moment-resisting frames (SMF), special concentrically braced frames (SCBF), and eccentrically braced frames (EBF) are the most commonly employed in seismic design codes, including ASCE 7-22 (American Society of Civil Engineers, 2022) and Iran's Standard 2800 (Road, Housing and Urban Development Research Center, 2026).

However, the collapse behavior of these three systems follows different mechanisms: SMF dissipates energy through the formation of plastic hinges at beam-column connections, EBF through shear yielding of the link beam, and SCBF through buckling and post-buckling of braces (Uriz & Mahin, 2004; Uriz, 2005; Uriz et al., 2008; Popov & Engelhardt, 1988; Kasai & Popov, 1986; Malley & Popov, 1983; Ricles & Popov, 1987; Mansour et al., 2011; Shen et al., 2011; Malakoutian et al., 2013; Mortazavi et al., 2023a, 2023b; Guo et al., 2024, 2025; Tong & Wang, 2024; Zhang et al., 2020a, 2020b, 2023; Men et al., 2022; Cheng et al., 2020; Yao et al., 2020; Özkılıç & Topkaya, 2021).

Previous studies have primarily focused on evaluating the seismic performance of each of these systems individually (Hamidia et al., 2022; Wang et al., 2022; Liapopoulou et al., 2024; Lilliefors, 1967; Azhari & Hamidia, 2025; Jamshidian et al., 2024; Zamani et al., 2024a, 2024b; Ding et al., 2025; Asjodi & Dolatshahi, 2023; Rezaei et al., 2023). Some research has also investigated the effects of parameters such as number of stories, period, and seismic hazard level on CMR (Rashvand et al., 2025a, 2025b; Zareian et al., 2010; Kircher et al., 2010; Lignos et al., 2011; Lignos & Krawinkler, 2013; Lignos & Krawinkler, 2011). However, a consistent, data-driven statistical comparison among the three aforementioned systems, while controlling

for confounding variables such as hazard level and design methodology, has received less attention in the literature.

This research gap becomes particularly significant given that the choice of structural system during the preliminary design phase directly impacts seismic safety (Nakashima et al., 2000; Ghobarah, 2001; Shirpour et al., 2024; Bakhshivand et al., 2022; Kiani et al., 2024; Shirpour & Fanaie, 2024; Hadinejad et al., 2025).

The novelty of the present paper lies in two main axes: first, the application of inferential statistical methods including one-way analysis of variance (ANOVA) (St & Wold, 1989; Kim, 2014; Henson, 2015; Kaufmann & Schering, 2007; Larson, 2008), Tukey's test, and their non-parametric counterparts (Kruskal–Wallis and Mann–Whitney) (McKight & Najab, 2010; Okoye & Hosseini, 2024; Chicco et al., 2025) to validate the results; second, the provision of quantitative effect size measures (η^2) that facilitate the practical interpretation of findings for application in the revision of design provisions. In this paper, following the introduction of the data and statistical methodology, the results of comparing CMR among the three systems SMF, SCBF, and EBF are presented, and the physical interpretation of the findings is discussed based on the behavioral mechanisms of each system. Finally, the practical implications of the results for seismic design and suggestions for future research are presented. Figure 1 depicts the general workflow of this research.

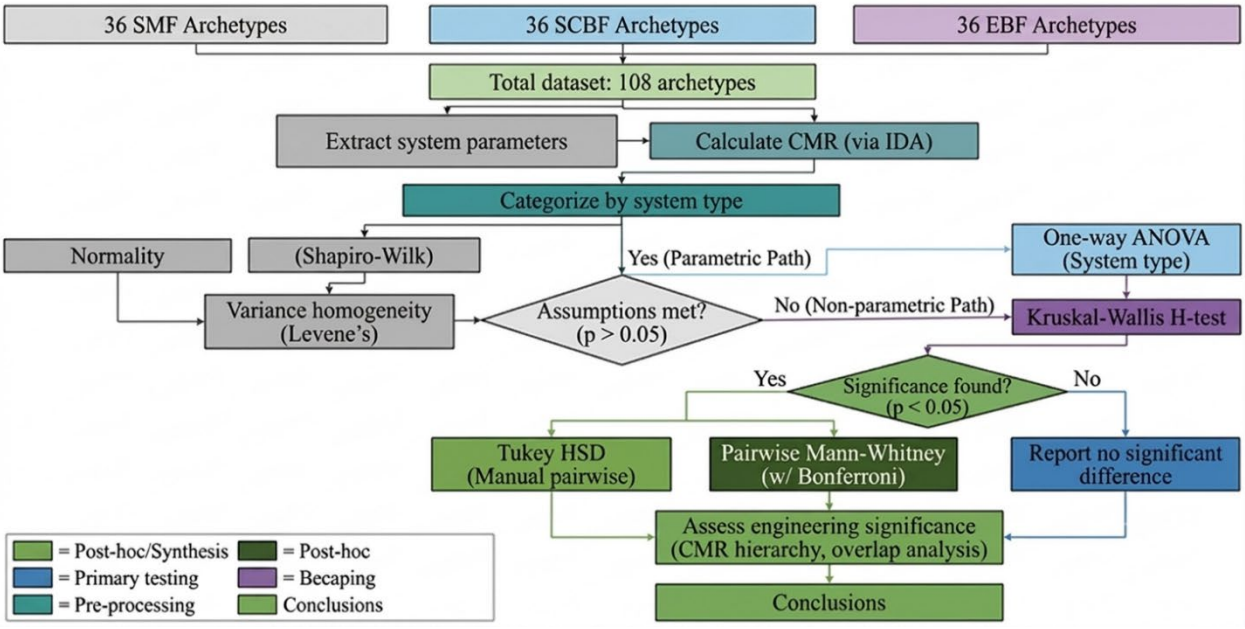

Figure 1. Methodological framework for comparative CMR analysis across steel lateral load-carrying systems.

2. Database Description and Building Archetypes

The database used in this paper is extracted from various peer-reviewed scientific articles, comprising 108 samples of steel archetypes (Federal Emergency Management Agency, 2009; American Society of Civil Engineers, 2022; Kircher et al., 2010; Pacific Earthquake Engineering Research Center, 2010; Baker, 2007). Each sample corresponds to a structural archetype that has been evaluated using the framework established in the FEMA P-695 methodology. Developed by the Federal Emergency Management Agency of the United States, FEMA P-695 provides a comprehensive framework for evaluating the seismic performance of structural systems and calibrating seismic design coefficients. Within this framework, a set of prototype structures referred to as "archetypes" is defined, systematically covering the design space of each structural system. Each archetype is subjected to incremental dynamic analysis using a standard set of earthquake ground motion records to determine the spectral acceleration corresponding to median collapse (SCT). The ratio of this quantity to the spectral acceleration at the design hazard level (SMT) constitutes the Collapse Margin Ratio (CMR), which is the primary measure of collapse safety.

The initial database comprised 108 steel archetypes with three different lateral load-resisting systems. A preliminary data review revealed that six archetypes had SMT values different from the others. Since CMR is directly dependent on SMT, the presence of different hazard levels in the sample could confound comparisons among the systems. Accordingly, these six archetypes were removed from the analysis, and 102 archetypes with an identical hazard level (SMT = 0.5g) were selected as the final sample. This filtering ensures that any observed differences in CMR are attributed solely to the structural system type and not to variations in seismic hazard level.

The final sample is balanced across the three structural systems: special moment-resisting frames, special concentrically braced frames, and eccentrically braced frames, each with 36 archetypes (Figure 2). This balanced distribution is a fundamental prerequisite for the statistical tests employed in this paper and enhances the validity of the statistical comparisons. The archetypes of each system exhibit considerable diversity in terms of geometric and design parameters. The number of stories ranges from 1 to 14, and structural heights span from 3.8 to 53.2 meters. The fundamental period (T1) also varies from 0.1 to 1.4 seconds, covering a broad range of dynamic behavior. Structural weights range from 4,500 to 63,000 kN, and design base shears vary from 675 to 9,450 kN. Figure 2 illustrates the relationship between design base shear and building height for all 108 archetypes, demonstrating the broad range of designs captured in the database. This diversity in design parameters provides a reasonable representation of the actual design space for each system. Complete specifications of the archetypes are presented in Table 1.

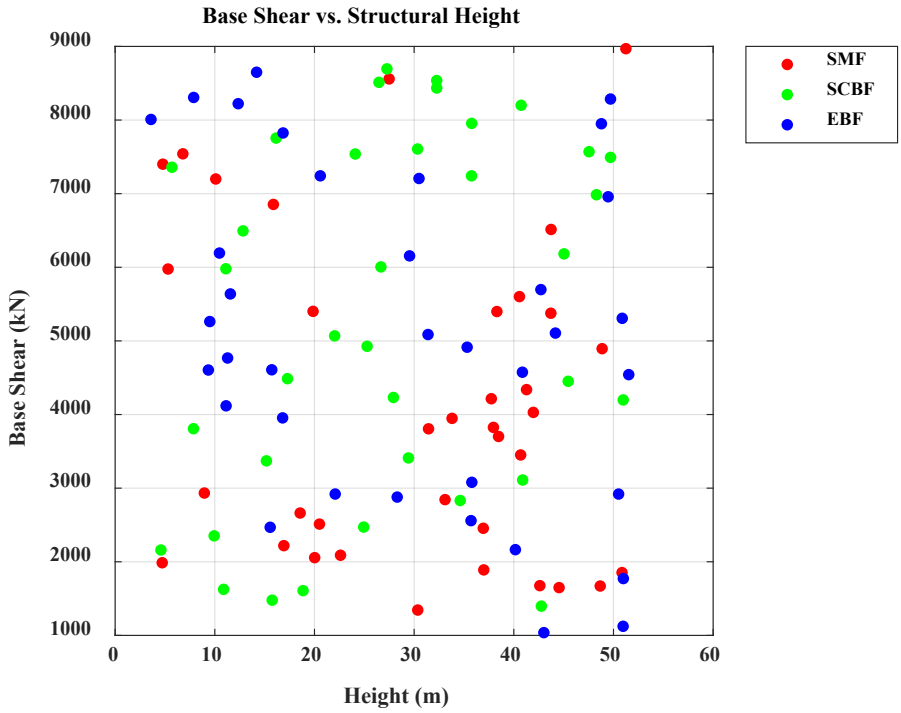

Figure 2. Relationship between design base shear and building height for steel structural archetypes.

In terms of design methodology, the archetypes are designed using two approaches: the equivalent lateral force (ELF) and the response spectrum analysis (RSA) procedures. Additionally, two seismic design categories, D_{min} and D_{max}, are present in the sample, representing moderate and high seismicity regions, respectively. The distribution of these variables is identical across all three systems, enabling a more controlled comparison. It should be noted that in this research, design methodology and seismic design category are considered control variables, and the primary focus of the analysis is on the effect of structural system type.

The primary dependent variable in this paper is the collapse margin ratio. This index indicates how many times the design hazard level spectral acceleration a structure can withstand before collapse occurs. Higher CMR values indicate a greater safety margin in contradiction of collapse. Descriptive statistics of CMR for all three systems are presented in Table 2. The mean CMR values for SMF, SCBF, and EBF are 2.34, 2.06, and 1.79, respectively, indicating a gradual decrease in collapse margin from SMF to EBF. Figure 3 presents the mean CMR along with the associated standard deviation for each system type, providing a visual summary of the descriptive statistics reported in Table 2. However, determining the statistical significance of these differences requires the application of inferential tests, which will be described in the methodology section.

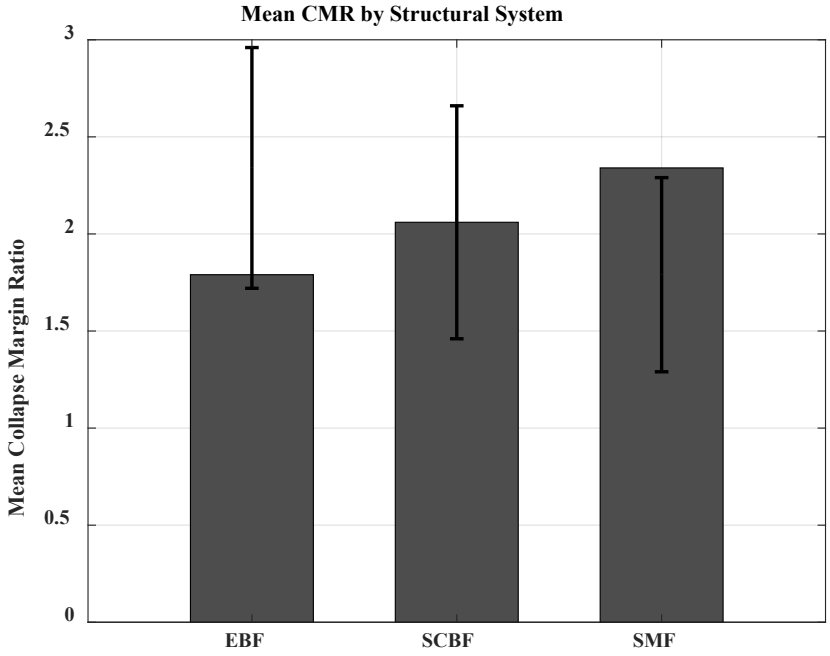

Figure 3. Mean collapse margin ratio and associated standard deviation by system type.

Table 1. Summary of structural archetype characteristics and design parameters.

System Type	Total Archetypes (n)	Height Range (m)	Period Range (T_1, sec)	Design Method (RSA/ELF)
SMF	36	3.8 – 53.2	0.2 – 1.4	18 / 18
SCBF	36	3.8 – 53.2	0.1 – 1.4	18 / 18
EBF	36	3.8 – 53.2	0.1 – 1.4	18 / 18

Table 2. Descriptive statistics of collapse margin ratio across steel structural systems.

Statistic	SMF	SCBF	EBF
Mean CMR	2.34	2.06	1.79
Std. Deviation	0.62	0.6	0.5
Minimum	1.22	1.02	1.07
Maximum	3.31	2.98	2.95

3. Methodology

The primary objective of this research is the statistical comparison of the CMR among three steel structural systems. To achieve this goal, a two-step approach is adopted: first, the statistical assumptions required for parametric tests are verified, and then, based on the results of this verification, appropriate tests are selected and performed. All statistical calculations are carried out using the Python programming language and the SciPy and NumPy libraries.

3.1. Verification of Statistical Assumptions

Prior to performing the analysis of variance, two fundamental assumptions must be satisfied: normality of data distribution within each group and homogeneity of variances across groups. To assess the normality of CMR distribution in each system, the Shapiro–Wilk test is employed. Compared to other normality tests such as Kolmogorov–Smirnov, this test has greater statistical power for sample sizes smaller than 50, making it a suitable choice for a sample size of 36 per group. The null hypothesis of this test states that the distribution is normal, and failure to reject it at a significance level of 0.05 is considered confirmation of the normality assumption. To examine the homogeneity of variances, Levene's test (Schultz, 1985; Gastwirth et al., 2009; Nordstokke & Zumbo, 2010) is used. This test is more robust to deviations from normality than Bartlett's test and is more widely applied in engineering studies where data may not be perfectly normally distributed. Failure to reject the null hypothesis at a significance level of 0.05 indicates homogeneity of variances and confirms this assumption for performing ANOVA.

3.2. One-Way Analysis of Variance

After confirming the statistical assumptions, one-way ANOVA is used to examine the significance of differences in mean CMR among the three systems. In this test, the independent variable is the structural system type (SMF, SCBF, EBF), and the dependent variable is CMR. The null hypothesis states that the mean CMR is equal across all three groups. The resulting F-statistic in ANOVA represents the ratio of between-group variance to within-group variance, and a high value indicates that the observed differences exceed the random variability within each group. In addition to statistical significance, the effect size is also calculated using the eta-squared (η^2) index. This index indicates what proportion of the total variance in CMR is explained by the structural system type. According to conventional benchmarks, η^2 values of 0.01, 0.06, and 0.14 represent small, medium, and large effect sizes, respectively.

3.3. Tukey's Post-Hoc Test

ANOVA only indicates the overall significance of differences among groups and does not specify which pairs of groups differ significantly from one another. For this purpose, Tukey’s honestly significant difference (HSD) post-hoc test is employed. This test performs all pairwise comparisons simultaneously and, by controlling the family-wise Type I error rate, minimizes

the probability of false conclusions. The q-statistic in this test is obtained by dividing the mean difference between two groups by the pooled standard error and is compared with the critical value from the studentized range distribution.

3.4. Non-Parametric Tests

To enhance the robustness of the results and validate the parametric findings, equivalent non-parametric tests are also performed. The Kruskal–Walli's test is used as the non-parametric counterpart of ANOVA, and the Mann–Whitney U test with Bonferroni correction is employed as the non-parametric counterpart for pairwise comparisons. These tests operate based on data ranking and are not dependent on data distribution. Agreement between parametric and non-parametric results provides greater confidence in the validity of the research's conclusions. In the Bonferroni correction, the significance level for each pairwise test is set to α/k, where k is the number of pairwise comparisons (equal to 3).

4. Results

In this section, the results obtained from the statistical tests introduced in the Methodology section are presented in detail. The order of presentation follows the logical sequence of the tests: first, confirmation of statistical assumptions; second, ANOVA results and effect size; and finally, pairwise comparisons and non-parametric validation.

4.1. Confirmation of Statistical Assumptions

The results of the Shapiro–Wilk test for all three groups indicated that the distribution of CMR in none of the systems deviated significantly from normality. The W-statistic values for SMF, SCBF, and EBF are 0.944, 0.940, and 0.944, respectively, and the p-values for all three tests are greater than 0.05 ($p = 0.065$, $p = 0.051$, $p = 0.066$, respectively). Therefore, the null hypothesis of normality is not rejected for any of the three groups, and the normality assumption is confirmed. Figure 4 presents the statistical distribution of CMR across the three structural systems, providing a visual complement to the Shapiro-Wilk test results. The results of Levene's test also showed that the variances of CMR among the three systems are homogeneous ($F = 1.99$, $p = 0.1423$). Failure to reject the null hypothesis in this test confirms that the homogeneity of variances assumption holds, and performing ANOVA is statistically justified from this perspective. The complete results of these tests are presented in Table 3.

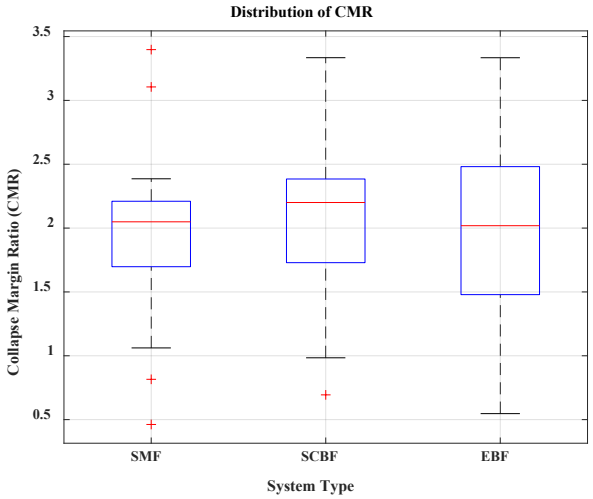

Figure 4. Statistical validation of variance homogeneity and system performance differences.

Table 3. Statistical validation of variance homogeneity and system performance differences.

Test	Statistic	p-value	Conclusion
ANOVA	F = 8.19	0.0005	Significant
Kruskal-Wallis	H = 13.91	0.0009	Significant
Levene's Test	F = 1.99	0.1423	Variance Equal

4.2. One-Way Analysis of Variance Results

The ANOVA results indicated that the difference in mean CMR among the three structural systems is statistically significant (F = 8.19, p = 0.0005). This p-value is well below the 0.01 significance threshold, indicating that the probability of observing these differences by chance is very low. In other words, the structural system type has a significant effect on the collapse margin. The effect size index η^2 is calculated to be 0.135. According to Cohen's benchmarks, this value falls in the range of medium to large effect size, indicating that the structural system type alone explains 13.5% of the total variability in CMR. This finding is significant from an engineering perspective because it demonstrates that the choice of lateral load-resisting system, independent of other design parameters such as height and design method, contributes substantially to determining the collapse capacity of the structure.

4.3. Tukey's Post-Hoc Test Results

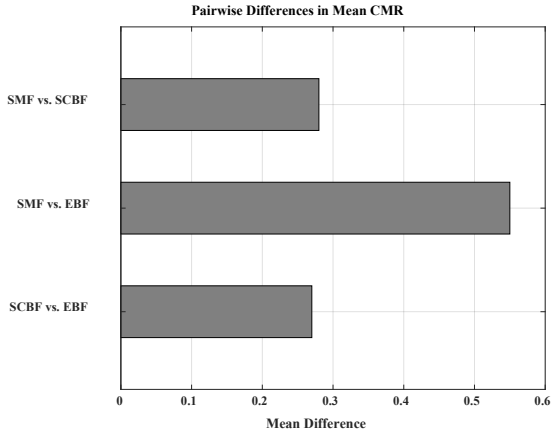

Figure 5. Post-Hoc pairwise comparison of collapse margin ratio across structural systems.

In contrast, the differences in mean CMR between SMF and SCBF (mean difference = 0.28, q = 2.89) and between SCBF and EBF (mean difference = 0.27, q = 2.75) are not statistically significant. This result indicates that SCBF occupies an intermediate position in terms of collapse margin between SMF and EBF, but its difference from neither of the other two systems reaches statistical significance. The results of the pairwise comparisons are presented in Table 4.

Table 4. Post-Hoc pairwise comparison of collapse margin ratio across structural systems.

Pairwise Comparison	Mean Diff	q (Tukey)	Significance
SMF vs. SCBF	0.28	2.89	$p > 0.05$
SMF vs. EBF	0.55	5.64	$p < 0.05$
SCBF vs. EBF	0.27	2.75	$p > 0.05$

4.4. Non-Parametric Validation

The results of the Kruskal–Wallis test confirmed that the difference among the three systems is statistically significant ($H = 13.91$, $p = 0.001$). This result is in complete agreement with the ANOVA findings and demonstrates that the significance of the differences is not dependent on the normality assumption. In the pairwise comparisons using the Mann–Whitney U test with Bonferroni correction, only the difference between SMF and EBF remained significant ($U = 972$, $p\_bonf = 0.001$). The differences for SMF-SCBF and SCBF-EBF are not significant after Bonferroni correction, which is perfectly consistent with the Tukey test results. The complete agreement between parametric and non-parametric results provides high confidence in the accuracy and robustness of the findings of this paper.

5. Discussion

The results of the statistical analyses in this research demonstrated that the structural system type has a significant effect on the collapse margin, with SMF exhibiting superior performance compared to EBF. In this section, these findings are interpreted from the perspective of the behavioral mechanisms of each system and compared with the existing literature (Figure 6).

5.1. Physical Interpretation of SMF Superiority

Special steel moment frames dissipate seismic energy through the formation of plastic hinges at the beam ends. This mechanism is inherently stable; after yielding, beams retain their load-carrying capacity, and positive strain-hardening behavior prevents sudden strength degradation. The widespread distribution of plastic hinges across different stories spreads the input seismic energy over a larger volume of the structure and prevents deformation concentration in any single story. This feature represents a significant advantage during long-duration earthquakes or near-field ground motions, where cumulative energy dissipation capacity becomes more critical. The mean CMR of 2.34 for SMF indicates that these structures can withstand, on average, 2.34 times the design spectral acceleration before collapse, representing an acceptable safety margin well above the minimum requirement of FEMA P-695.

5.2. Physical Interpretation of EBF Performance

Eccentrically braced frames dissipate energy through shear or flexural yielding of the link beam. The link beam is designed as a sacrificial element that exhibits stable cyclic behavior after yielding. However, the concentration of deformation in this limited element can lead to local damage and reduced lateral load-carrying capacity under severe earthquakes. Furthermore, the design of EBF based on the link yielding mechanism requires other members to be designed with high overstrength factors, resulting in greater stiffness and lower lateral ductility compared to SMF. The mean CMR of 1.79 for EBF, although above the minimum FEMA P-695 requirement, indicates a lower safety margin compared to SMF.

5.3. Physical Interpretation of SCBF Performance

Special concentrically braced frames initially rely on the buckling resistance of compression braces. After buckling, the system behavior changes dramatically; the buckled brace loses its compressive capacity, and the lateral load is primarily carried by the tension brace. This asymmetric behavior in tension-compression cycles provides lower energy dissipation compared to SMF. However, proper design of connections and non-braced members can prevent damage propagation and collapse. The intermediate position of SCBF, with a mean CMR of 2.06, is fully consistent with this physical interpretation.

5.4. Practical Implications

The findings of this research have direct implications for seismic design. First, the selection of a lateral load-resisting system should not be based solely on economic or architectural considerations; the significant difference in CMR between SMF and EBF demonstrates that this choice has measurable consequences for seismic safety. Second, the seismic performance factors (R, Ω_0, and C_d) specified in design codes, which are defined differently for each system, reflect these behavioral differences, but the results of this research indicate that these coefficients do not necessarily lead to equivalent collapse margins. Third, in projects where maximum collapse safety is desired, SMF is the superior choice, whereas EBF still provides an acceptable safety margin above code requirements in situations where architectural constraints make moment frame implementation difficult.

5.5. Research Limitations

The limitations of this research should also be noted. The data used are extracted from peer-reviewed articles, which are developed based on specific modeling assumptions and may not fully represent the actual behavior of all steel structures. Furthermore, the present analysis did not separately examine the effects of variables such as plan irregularities, P-Delta effects (Vandepitte, 1982; Adam et al., 2004; Bernal, 1987; Williamson, 2003; Bohlouli & Poursha, 2024; Dolatshahi et al., 2019; Zahrai & Hamidia, 2010; Zinati et al., 2026), and connection details. Future research can provide a more comprehensive picture of the factors influencing CMR by expanding the database and incorporating these variables.

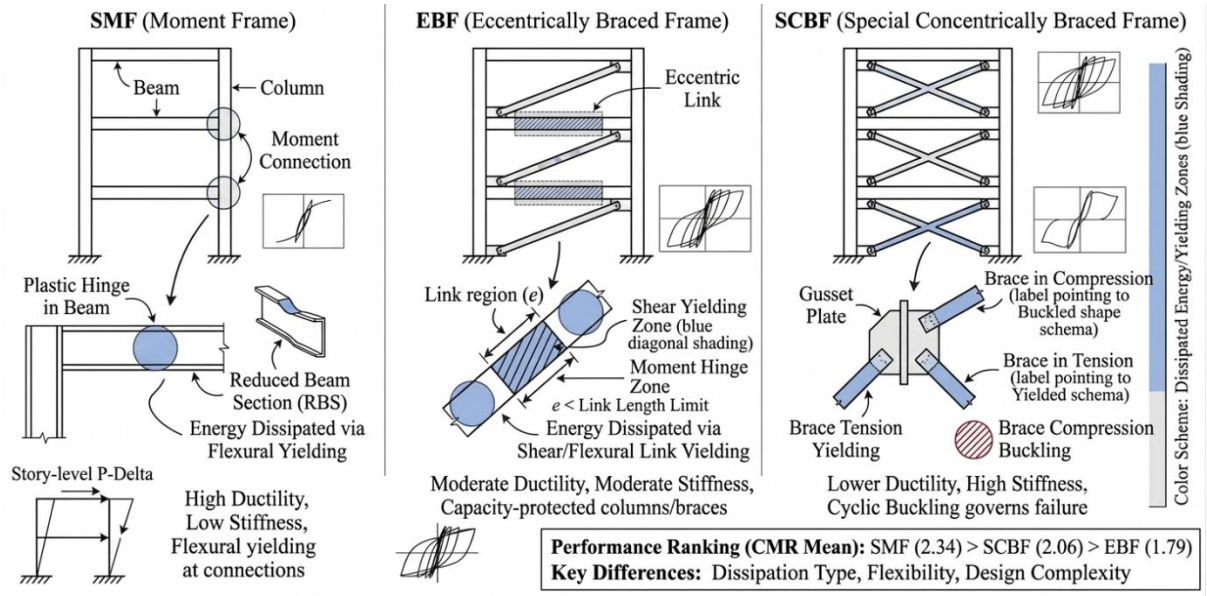

Figure 6. Comparative representation of steel seismic force-resisting systems and energy dissipation mechanisms.

6. Summary and Conclusion

This research is conducted with the aim of statistically comparing the collapse capacity of three common steel lateral load-resisting systems—special moment-resisting frames (SMF), special concentrically braced frames (SCBF), and eccentrically braced frames (EBF)—using the collected database from a relatively large number of peer-reviewed articles. From a total of 108 available archetypes, 108 samples with an identical hazard level (S_{MT} = 0.5g) are selected and analyzed using parametric and non-parametric statistical methods. The main novelty of this paper lies in its use of an inferential statistical approach for comparing the systems—an approach that has received less attention in previous studies in the literature. The simultaneous confirmation of normality and homogeneity of variance assumptions ensured the validity of the parametric tests, and the agreement of the results with non-parametric tests further reinforced the robustness of the findings. The results demonstrated that the choice of lateral load-resisting system—independent of structural height and design method—has a direct and measurable consequence on the safety margin against collapse; a finding with direct practical implications for revising system selection criteria in Iran's seismic design codes.

1. The structural system type has a significant effect on CMR ($F = 8.19$, $p < 0.001$); the lateral load-resisting system alone explains 13.5% of the total variability in collapse margin ($\eta^2 = 0.135$).
2. The mean CMR values for SMF, SCBF, and EBF are 2.34, 2.06, and 1.79, respectively; SMF exhibits a 31% higher collapse margin compared to EBF.
3. Only the difference between SMF and EBF is statistically significant ($q = 5.64$, $p < 0.05$); SCBF occupies an intermediate position, but its difference from neither of the other two systems reaches statistical significance.
4. The results of non-parametric tests (Kruskal–Wallis: $H = 13.91$, $p = 0.001$; Mann–Whitney with Bonferroni correction) are fully consistent with the parametric findings, confirming the robustness of the results.
5. The superiority of CMR in SMF is physically justified by its distributed energy dissipation mechanism through beam plastic hinges, implying that the selection of a lateral load-resisting system should be considered as a parameter affecting collapse safety in the early stages of design.

Appendix A

Table A1. Summary of design parameters and collapse performance indicators for the selected steel building archetypes.

Model ID	Stories	Height (m)	T_1 (sec)	Weight (kN)	Base Shear (kN)	Design Method	SDC	S_{CT}	S_{MT}	CMR	System Type
SMF 001	6	22.8	0.6	27000	4050	ELF	D_{min}	1.2343	0.5	2.47	SMF

SMF 002	5	19	0.5	22500	3375	RSA	D_{min}	0.75937	0.5	1.52	SMF
SMF 003	14	53.2	1.4	63000	9450	RSA	D_{max}	0.61132	0.5	1.22	SMF
SMF 004	4	15.2	0.4	18000	2700	ELF	D_{min}	1.11833	0.5	2.24	SMF
SMF 005	11	41.8	1.1	49500	7425	RSA	D_{max}	1.65704	0.5	3.31	SMF
SMF 006	6	22.8	0.6	27000	4050	RSA	D_{max}	1.31791	0.5	2.64	SMF
SMF 007	3	11.4	0.3	13500	2025	RSA	D_{min}	0.848	0.5	1.70	SMF
SMF 008	4	15.2	0.4	18000	2700	RSA	D_{max}	1.53172	0.5	3.06	SMF
SMF 009	14	53.2	1.4	63000	9450	RSA	D_{max}	1.58296	0.5	3.17	SMF
SMF 010	4	15.2	0.4	18000	2700	ELF	D_{max}	0.92841	0.5	1.86	SMF
SMF 011	6	22.8	0.6	27000	4050	ELF	D_{max}	1.04964	0.5	2.10	SMF
SMF 012	12	45.6	1.2	54000	8100	RSA	D_{max}	1.20526	0.5	2.41	SMF
SMF 013	14	53.2	1.4	63000	9450	ELF	D_{max}	1.59533	0.5	3.19	SMF
SMF 014	5	19	0.5	22500	3375	ELF	D_{min}	0.8281	0.5	1.66	SMF
SMF 015	10	38	1	45000	6750	ELF	D_{max}	0.76187	0.5	1.52	SMF
SMF 016	3	11.4	0.3	13500	2025	ELF	D_{max}	0.64797	0.5	1.30	SMF
SMF 017	7	26.6	0.7	31500	4725	RSA	D_{min}	0.96773	0.5	1.94	SMF
SMF 018	5	19	0.5	22500	3375	RSA	D_{min}	0.80794	0.5	1.62	SMF
SMF 019	12	45.6	1.2	54000	8100	RSA	D_{min}	0.81746	0.5	1.63	SMF
SMF 020	5	19	0.5	22500	3375	ELF	D_{min}	1.55128	0.5	3.10	SMF
SMF 021	6	22.8	0.6	27000	4050	RSA	D_{min}	0.70648	0.5	1.41	SMF
SMF 022	4	15.2	0.4	18000	2700	RSA	D_{min}	1.62084	0.5	3.24	SMF
SMF 023	6	22.8	0.6	27000	4050	ELF	D_{max}	1.50592	0.5	3.01	SMF
SMF 024	13	49.4	1.3	58500	8775	ELF	D_{min}	1.10225	0.5	2.20	SMF
SMF 025	8	30.4	0.8	36000	5400	ELF	D_{min}	0.83908	0.5	1.68	SMF
SMF 026	9	34.2	0.9	40500	6075	RSA	D_{max}	1.37001	0.5	2.74	SMF
SMF 027	2	7.6	0.2	9000	1350	RSA	D_{min}	1.35474	0.5	2.71	SMF
SMF 028	1	3.8	0.1	4500	675	RSA	D_{max}	1.45664	0.5	2.91	SMF

SMF 029	9	34.2	0.9	40500	6075	ELF	D_{max}	1.28189	0.5	2.56	SMF
SMF 030	11	41.8	1.1	49500	7425	ELF	D_{min}	1.32368	0.5	2.65	SMF
SMF 031	9	34.2	0.9	40500	6075	ELF	D_{min}	1.38787	0.5	2.78	SMF
SMF 032	13	49.4	1.3	58500	8775	RSA	D_{min}	1.38627	0.5	2.77	SMF
SMF 033	3	11.4	0.3	13500	2025	RSA	D_{min}	1.12797	0.5	2.26	SMF
SMF 034	3	11.4	0.3	13500	2025	ELF	D_{max}	1.3182	0.5	2.64	SMF
SMF 035	4	15.2	0.4	18000	2700	ELF	D_{max}	1.36033	0.5	2.72	SMF
SMF 036	3	11.4	0.3	13500	2025	RSA	D_{min}	1.17882	0.5	2.36	SMF
SCBF 001	13	49.4	1.3	58500	8775	RSA	D_{max}	0.76475	0.5	1.53	SCBF
SCBF 002	1	3.8	0.1	4500	675	ELF	D_{max}	1.07706	0.5	2.15	SCBF
SCBF 003	2	7.6	0.2	9000	1350	ELF	D_{min}	0.61439	0.5	1.23	SCBF
SCBF 004	6	22.8	0.6	27000	4050	ELF	D_{max}	1.3539	0.5	2.71	SCBF
SCBF 005	7	26.6	0.7	31500	4725	ELF	D_{max}	1.03327	0.5	2.07	SCBF
SCBF 006	4	15.2	0.4	18000	2700	ELF	D_{min}	0.98233	0.5	1.96	SCBF
SCBF 007	14	53.2	1.4	63000	9450	ELF	D_{max}	0.50938	0.5	1.02	SCBF
SCBF 008	14	53.2	1.4	63000	9450	ELF	D_{min}	0.68316	0.5	1.37	SCBF
SCBF 009	1	3.8	0.1	4500	675	ELF	D_{max}	1.28121	0.5	2.56	SCBF
SCBF 010	11	41.8	1.1	49500	7425	RSA	D_{min}	0.83732	0.5	1.67	SCBF
SCBF 011	4	15.2	0.4	18000	2700	ELF	D_{max}	0.94531	0.5	1.89	SCBF
SCBF 012	9	34.2	0.9	40500	6075	ELF	D_{max}	1.34913	0.5	2.70	SCBF
SCBF 013	9	34.2	0.9	40500	6075	RSA	D_{max}	1.44776	0.5	2.90	SCBF
SCBF 014	5	19	0.5	22500	3375	ELF	D_{max}	1.16714	0.5	2.33	SCBF
SCBF 015	6	22.8	0.6	27000	4050	ELF	D_{min}	1.27633	0.5	2.55	SCBF
SCBF 016	10	38	1	45000	6750	RSA	D_{min}	0.78935	0.5	1.58	SCBF
SCBF 017	10	38	1	45000	6750	ELF	D_{min}	1.44718	0.5	2.89	SCBF
SCBF 018	6	22.8	0.6	27000	4050	RSA	D_{max}	0.93964	0.5	1.88	SCBF
SCBF 019	6	22.8	0.6	27000	4050	ELF	D_{min}	1.19032	0.5	2.38	SCBF

SCBF020	7	26.6	0.7	31500	4725	ELF	D_{max}	1.35616	0.5	2.71	SCBF
SCBF021	2	7.6	0.2	9000	1350	RSA	D_{max}	1.26772	0.5	2.54	SCBF
SCBF022	14	53.2	1.4	63000	9450	ELF	D_{max}	0.73476	0.5	1.47	SCBF
SCBF023	6	22.8	0.6	27000	4050	ELF	D_{min}	1.47878	0.5	2.96	SCBF
SCBF024	5	19	0.5	22500	3375	ELF	D_{min}	1.11398	0.5	2.23	SCBF
SCBF025	8	30.4	0.8	36000	5400	ELF	D_{min}	1.08309	0.5	2.17	SCBF
SCBF026	2	7.6	0.2	9000	1350	ELF	D_{max}	0.73769	0.5	1.48	SCBF
SCBF027	5	19	0.5	22500	3375	RSA	D_{max}	0.70727	0.5	1.41	SCBF
SCBF028	13	49.4	1.3	58500	8775	ELF	D_{min}	1.4895	0.5	2.98	SCBF
SCBF029	13	49.4	1.3	58500	8775	RSA	D_{min}	0.60367	0.5	1.21	SCBF
SCBF030	1	3.8	0.1	4500	675	ELF	D_{max}	0.93206	0.5	1.86	SCBF
SCBF031	3	11.4	0.3	13500	2025	ELF	D_{min}	0.57621	0.5	1.15	SCBF
SCBF032	11	41.8	1.1	49500	7425	ELF	D_{min}	0.79056	0.5	1.58	SCBF
SCBF033	1	3.8	0.1	4500	675	RSA	D_{max}	1.26032	0.5	2.52	SCBF
SCBF034	1	3.8	0.1	4500	675	RSA	D_{min}	1.22468	0.5	2.45	SCBF
SCBF035	12	45.6	1.2	54000	8100	RSA	D_{min}	0.62543	0.5	1.25	SCBF
SCBF036	6	22.8	0.6	27000	4050	RSA	D_{min}	1.38416	0.5	2.77	SCBF
EBF001	5	19	0.5	22500	3375	RSA	D_{max}	1.3323	0.5	2.66	EBF
EBF002	14	53.2	1.4	63000	9450	RSA	D_{max}	1.02369	0.5	2.05	EBF
EBF003	11	41.8	1.1	49500	7425	ELF	D_{max}	0.99487	0.5	1.99	EBF
EBF004	8	30.4	0.8	36000	5400	ELF	D_{min}	1.17395	0.5	2.35	EBF
EBF005	9	34.2	0.9	40500	6075	ELF	D_{max}	0.90119	0.5	1.80	EBF
EBF006	14	53.2	1.4	63000	9450	RSA	D_{max}	0.64607	0.5	1.29	EBF
EBF007	7	26.6	0.7	31500	4725	RSA	D_{min}	0.75693	0.5	1.51	EBF
EBF008	4	15.2	0.4	18000	2700	RSA	D_{min}	0.81054	0.5	1.62	EBF
EBF009	4	15.2	0.4	18000	2700	RSA	D_{max}	1.00041	0.5	2.00	EBF
EBF010	5	19	0.5	22500	3375	RSA	D_{max}	0.90698	0.5	1.81	EBF

EBF011	8	30.4	0.8	36000	5400	ELF	D_{min}	0.71632	0.5	1.43	EBF
EBF012	14	53.2	1.4	63000	9450	RSA	D_{min}	1.30053	0.5	2.60	EBF
EBF013	2	7.6	0.2	9000	1350	ELF	D_{max}	1.07342	0.5	2.15	EBF
EBF014	11	41.8	1.1	49500	7425	ELF	D_{min}	0.53328	0.5	1.07	EBF
EBF015	8	30.4	0.8	36000	5400	RSA	D_{min}	0.63759	0.5	1.28	EBF
EBF016	13	49.4	1.3	58500	8775	ELF	D_{max}	0.71822	0.5	1.44	EBF
EBF017	14	53.2	1.4	63000	9450	ELF	D_{max}	1.03699	0.5	2.07	EBF
EBF018	8	30.4	0.8	36000	5400	RSA	D_{max}	0.99512	0.5	1.99	EBF
EBF019	13	49.4	1.3	58500	8775	ELF	D_{min}	0.76445	0.5	1.53	EBF
EBF020	12	45.6	1.2	54000	8100	RSA	D_{min}	0.65592	0.5	1.31	EBF
EBF021	12	45.6	1.2	54000	8100	ELF	D_{max}	0.62854	0.5	1.26	EBF
EBF022	8	30.4	0.8	36000	5400	RSA	D_{min}	0.98459	0.5	1.97	EBF
EBF023	10	38	1	45000	6750	RSA	D_{max}	1.2237	0.5	2.45	EBF
EBF024	14	53.2	1.4	63000	9450	ELF	D_{min}	0.9471	0.5	1.89	EBF
EBF025	8	30.4	0.8	36000	5400	ELF	D_{max}	0.94777	0.5	1.90	EBF
EBF026	6	22.8	0.6	27000	4050	ELF	D_{max}	1.47668	0.5	2.95	EBF
EBF027	5	19	0.5	22500	3375	ELF	D_{max}	0.54264	0.5	1.09	EBF
EBF028	5	19	0.5	22500	3375	ELF	D_{max}	0.63111	0.5	1.26	EBF
EBF029	5	19	0.5	22500	3375	ELF	D_{max}	0.68796	0.5	1.38	EBF
EBF030	6	22.8	0.6	27000	4050	ELF	D_{max}	0.80954	0.5	1.62	EBF
EBF031	8	30.4	0.8	36000	5400	RSA	D_{max}	0.60607	0.5	1.21	EBF
EBF032	9	34.2	0.9	40500	6075	RSA	D_{min}	0.93989	0.5	1.88	EBF
EBF033	7	26.6	0.7	31500	4725	ELF	D_{max}	0.60309	0.5	1.21	EBF
EBF034	1	3.8	0.1	4500	675	ELF	D_{min}	0.82784	0.5	1.66	EBF
EBF035	7	26.6	0.7	31500	4725	ELF	D_{max}	1.43512	0.5	2.87	EBF
EBF036	6	22.8	0.6	27000	4050	ELF	D_{min}	0.95093	0.5	1.90	EBF

7. References

Asjodi, A. H., & Dolatshahi, K. M. (2023). Extended fragility surfaces for unreinforced masonry walls using vision-derived damage parameters. *Engineering Structures, 278*, 115467.

Azhari, S., & Hamidia, M. (2025). Probabilistic postearthquake ASCE 41-17 compliant performance level identification for shear-dominated RC shear walls via crack image analysis. *Journal of Structural Engineering, 151*(1), 04024185.

American Society of Civil Engineers. (2022). *Minimum design loads and associated criteria for buildings and other structures (ASCE/SEI 7-22).*

Adam, C., Ibarra, L. F., & Krawinkler, H. (2004). Evaluation of P-delta effects in non-deteriorating MDOF structures from equivalent SDOF systems. Technical report, Pacific Earthquake Engineering Research Center.

Baker, J. W. (2007). Quantitative classification of near-fault ground motions using wavelet analysis. *Bulletin of the Seismological Society of America, 97*(5), 1486–1501.

Bernal, D. (1987). Amplification factors for inelastic dynamic P–Δ effects in earthquake analysis. *Earthquake Engineering & Structural Dynamics, 15*(5), 635–651.

Bakhshivand, E., Amiri, H. A., & Maleki, S. (2022). Evaluation of seismic performance factors for dual steel SMF-SCBF systems using FEMA P695 methodology. *Soil Dynamics and Earthquake Engineering, 163*, 107506.

Bohlouli, Z., & Poursha, M. (2024). Effects of P-delta and spectral shape of ground motion records on strength reduction factor and inelastic displacement ratio of SDOF systems with deterioration. *Structures, 69*, 107410.

Chen, C. H., Lai, J. W., & Mahin, S. (2008, April 24–26). Numerical modelling and performance assessment of concentrically braced steel frames. In *Structures Congress 2008: Crossing Borders* (pp. 1–10). American Society of Civil Engineers.

Chen, C. H., & Mahin, S. (2010, May 12–15). Seismic collapse performance of concentrically steel braced frames. In *Structures Congress 2010* (pp. 1265–1274). American Society of Civil Engineers.

Cheng, Q., Su, M., Lian, M., Zhang, H., Guan, B., & Gong, H. (2020). Cyclic behavior of high-strength steel framed-tube structures with bolted replaceable shear links. *Engineering Structures, 210*, 110395.

Coburn, A., & Spence, R. (2002). *Earthquake protection* (2nd ed.). John Wiley & Sons.

Chicco, D., Sichenze, A., & Jurman, G. (2025). A simple guide to the use of Student's t-test, Mann–Whitney U test, Chi-squared test, and Kruskal–Wallis test in biostatistics. *BioData Mining, 18*(1), 56.

Ding, J. W., Lu, D. G., & Cao, Z. G. (2025). Risk assessment of spatially distributed assets with generalized seismic fragility models based on machine learning. *Soil Dynamics and Earthquake Engineering, 198*, 109533.

Dolatshahi, K. M., Vafaei, A., Kildashti, K., & Hamidia, M. (2019). Displacement ratios for structures with material degradation and foundation uplift. *Bulletin of Earthquake Engineering, 17*(9), 5133–5157.

Federal Emergency Management Agency. (2009). *Quantification of building seismic performance factors (FEMA P-695).*

Guo, Y., Lian, M., & Cheng, Q. (2024). Performance-based plastic design of high-strength steel framed-tube structures fused with replaceable shear links. *Journal of Constructional Steel Research, 212*, 108291.

Guo, Y., Lian, M., & Su, M. (2025). Response modification factor of high-strength steel frame-tube structures with replaceable shear links. *Journal of Constructional Steel Research, 229*, 109510.

Ghobarah, A. (2001). Performance-based design in earthquake engineering: State of development. *Engineering Structures, 23*(8), 878–884.

Gastwirth, J. L., Gel, Y. R., & Miao, W. (2009). The impact of Levene's test of equality of variances on statistical theory and practice. *Statistical Science, 24*(3), 343–360.

Hamidia, M., Shokrollahi, N., & Ardakani, R. R. (2022). The collapse margin ratio of steel frames considering the vertical component of earthquake ground motions. *Journal of Constructional Steel Research, 188*, 107054.

Hadinejad, A., Asghari, A., & Marefat, M. S. (2025). Evaluation of FEMA P695 methodology for quantification of seismic performance factors in dual steel SCBF-SMF structures. *Structures, 71*, 108172.

Henson, R. N. (2015). Analysis of variance (ANOVA). In *Brain mapping* (pp. 477–481).

Jamshidian, S., Azhari, S., & Hamidia, M. (2024). Rapid post-earthquake loss quantification using crack patterns of reinforced concrete columns. *Structures, 69*, 107372.

Kasai, K., & Popov, E. P. (1986). *A study of seismically resistant eccentrically braced steel frame systems* (Report No. UCB/EERC-86/01). University of California, Berkeley.

Kiani, A., Yang, T. Y., Kheyroddin, A., Kafi, M. A., & Naderpour, H. (2024). Quantification of seismic performance factors of mixed concrete/steel buildings using FEMA P695 methodology. *Structures, 61*, 106144.

Kircher, C., Deierlein, G., Hooper, J., Krawinkler, H., Mahin, S., Shing, B., & Wallace, J. (2010). Evaluation of the FEMA P-695 methodology for quantification of building seismic performance factors. *Earthquake Spectra, 26*(4), 1012–1025.

Kircher, C., Deierlein, G., Hooper, J., Krawinkler, H., Mahin, S., Shing, B., & Wallace, J. (2010). Evaluation of the FEMA P-695 methodology for quantification of building seismic performance factors. *Earthquake Spectra, 26*(4), 1012–1025.

Kim, H. Y. (2014). Analysis of variance (ANOVA) comparing means of more than two groups. *Restorative Dentistry & Endodontics, 39*(1), 74–77.

Kaufmann, J., & Schering, A. G. (2007). Analysis of variance ANOVA. In *Wiley encyclopedia of clinical trials* (pp. 1–6).

Larson, M. G. (2008). Analysis of variance. *Circulation, 117*(1), 115–121.

Lignos, D. G., Krawinkler, H., & Whittaker, A. S. (2011). Prediction and validation of sidesway collapse of two scale models of a 4-story steel moment frame. *Earthquake Engineering & Structural Dynamics, 40*(7), 807–825.

Lignos, D. G., & Krawinkler, H. (2013). Development and utilization of structural component databases for performance-based earthquake engineering. *Journal of Structural Engineering, 139*(8), 1382–1394.

Lignos, D. G., & Krawinkler, H. (2011). Deterioration modeling of steel components in support of collapse prediction of steel moment frames under earthquake loading. *Journal of Structural Engineering, 137*(11), 1291–1302.

Liapopoulou, M., Stafford, P. J., & Elghazouli, A. Y. (2024). Duration-dependent seismic collapse capacity prediction for steel moment-resisting frames. *Journal of Building Engineering, 86*, 108810.

Lilliefors, H. W. (1967). On the Kolmogorov-Smirnov test for normality with mean and variance unknown. *Journal of the American Statistical Association, 62*(318), 399–402.

Liel, A. B., Haselton, C. B., & Deierlein, G. G. (2011). Seismic collapse safety of reinforced concrete buildings. II: Comparative assessment of nonductile and ductile moment frames. *Journal of Structural Engineering, 137*(4), 492–502.

Malley, J. O., & Popov, E. P. (1983). *Design considerations for shear links in eccentrically braced frames* (Report No. UCB/EERC-83/24). University of California, Berkeley.

Mansour, N., Christopoulos, C., & Tremblay, R. (2011). Experimental validation of replaceable shear links for eccentrically braced steel frames. *Journal of Structural Engineering, 137*(10), 1141–1152.

Malakoutian, M., Berman, J. W., & Dusicka, P. (2013). Seismic response evaluation of the linked column frame system. *Earthquake Engineering & Structural Dynamics, 42*(6), 795–814.

Men, J., Xiong, L., Wang, J., & Zhang, Q. (2022). Experimental and numerical study on the behavior of novel multi-segment replaceable steel shear links. *Journal of Constructional Steel Research, 194*, 107314.

Mortazavi, P., Lee, E., Binder, J., Kwon, O. S., & Christopoulos, C. (2023). Large-scale experimental validation of optimized cast steel replaceable modular yielding links for eccentrically braced frames. *Journal of Structural Engineering, 149*(7), 04023071.

Mortazavi, P., Binder, J., Kwon, O. S., & Christopoulos, C. (2023). Ductility-targeted design of cast steel replaceable modular yielding links and their experimental validation through large-scale testing. *Journal of Structural Engineering, 149*(7), 04023080.

McKight, P. E., & Najab, J. (2010). Kruskal–Wallis test. In *The Corsini encyclopedia of psychology*.

Nakashima, M., Roeder, C. W., & Maruoka, Y. (2000). Steel moment frames for earthquakes in United States and Japan. *Journal of Structural Engineering, 126*(8), 861–868.

Nordstokke, D. W., & Zumbo, B. D. (2010). A new nonparametric Levene test for equal variances. *Psicológica, 31*(2), 401–430.

Okoye, K., & Hosseini, S. (2024). Mann–Whitney U test and Kruskal–Wallis H test statistics in R. In *R programming: Statistical data analysis in research* (pp. 225–246). Springer Nature Singapore.

O'Reilly, G. J., Goggins, J., & Mahin, S. A. (2012, September 24–28). Behaviour and design of a self-centering concentrically braced steel frame system. Paper presented at the 15th World Conference on Earthquake Engineering, Lisbon, Portugal.

Özkılıç, Y. O., & Topkaya, C. (2021). Extended end-plate connections for replaceable shear links. *Engineering Structures, 240*, 112385.

Pacific Earthquake Engineering Research Center. (2010). *Guidelines for performance-based seismic design of tall buildings (PEER Report No. 2010/05).*

Popov, E. P., & Engelhardt, M. D. (1988). Seismic eccentrically braced frames. *Journal of Constructional Steel Research, 10*, 321–354.

Ricles, J. M., & Popov, E. P. (1987). *Experiments on eccentrically braced frames with composite floors* (Report No. UCB/EERC-87/06). University of California, Berkeley.

Rezaei, S., Dolatshahi, K. M., & Asjodi, A. H. (2023). Multivariable fragility curves for unreinforced masonry walls. *Bulletin of Earthquake Engineering, 21*(7), 3357–3398.

Rashvand, P., Hamidia, M. J., & Hassani, N. (2025). Assessment of seismic collapse capacity in special moment-resisting frames designed via equivalent lateral force and response spectrum procedures under ASCE 7-22 and FEMA P-695 frameworks. *Interdisciplinary Journal of Civil Engineering, 1*(4), 428–445.

Rashvand, P., Hamidia, M., & Hassani, N. (2025). Seismic collapse capacity assessment of steel special moment resisting frames designed based on equivalent lateral force and response spectrum analysis procedures according to ASCE 7–22 standard. Paper presented at the 14th International Congress of Civil Engineering, Tehran, Iran. Civilica. https://civilica.com/doc/2456268

Road, Housing and Urban Development Research Center. (2026). *Iranian code of practice for seismic resistant design of buildings (Standard No. 2800, 5th ed.).*

Schultz, B. B. (1985). Levene's test for relative variation. *Systematic Zoology, 34*(4), 449–456.

Shen, Y., Christopoulos, C., Mansour, N., & Tremblay, R. (2011). Seismic design and performance of steel moment-resisting frames with nonlinear replaceable links. *Journal of Structural Engineering, 137*(10), 1107–1117.

Shirpour, A., & Fanaie, N. (2024). Quantifying the seismic performance factors of half-elliptic-braced steel moment frames. *Engineering Structures, 311*, 118189.

Spence, R., & Coburn, A. (2006). Earthquake risk and insurance. In *Assessing and managing earthquake risk: Geo-scientific and engineering knowledge for earthquake risk mitigation* (pp. 385–402). Springer Netherlands.

Spence, R., So, E., Ameri, G., Akinci, A., Cocco, M., Cultrera, G., Pacor, F., Zonno, G., Franceschina, G., Marcucci, S., Milana, G., Di Pasquale, G., Lucantoni, A., Bramerini, F., Pitilakis, K., Kakderi, K., Anastasiadis,

A., Reis, S., Aydinoğlu, M., … Carvalho, A. (2007). Earthquake disaster scenario prediction and loss modelling for urban areas (LESSLOSS Report 7). LESSLOSS.

Shirpour, A., Fanaie, N., & Seraji, M. B. (2024). Seismic performance factors of quarter-elliptic-braced steel moment frames using FEMA P695 methodology. *Soil Dynamics and Earthquake Engineering, 178*, 108453.

St, L., & Wold, S. (1989). Analysis of variance (ANOVA). *Chemometrics and Intelligent Laboratory Systems, 6*(4), 259–272.

Tong, Y., & Wang, M. (2024). Experimental study on seismic performance of replaceable shear links with low-yield-point steel. *Journal of Constructional Steel Research, 222*, 108975.

Uriz, P., & Mahin, S. A. (2004, August 1–6). Seismic performance assessment of concentrically braced steel frames. Paper presented at the 13th World Conference on Earthquake Engineering, Vancouver, Canada.

Uriz, P., Mahin, S., Huang, Y., & Chen, C. H. (2006). Bracing for the future: What we know about concentrically braced steel frames. Technical report, Pacific Earthquake Engineering Research Center.

Uriz, P., Filippou, F. C., & Mahin, S. A. (2008). Model for cyclic inelastic buckling of steel braces. *Journal of Structural Engineering, 134*(4), 619–628.

Uriz, P. (2005). *Towards earthquake resistant design of concentrically braced steel structures* (Doctoral dissertation, University of California, Berkeley).

Vandepitte, D. (1982). Non-iterative analysis of frames including the P–Δ effect. *Journal of Constructional Steel Research, 2*(2), 3–10.

Wang, X., Zhang, X. A., Shahzad, M. M., & Shi, X. (2022). Fragility analysis and collapse margin capacity assessment of mega-sub controlled structure system under mainshock-aftershock sequences. *Journal of Building Engineering, 49*, 104080.

Williamson, E. B. (2003). Evaluation of damage and P–Δ effects for systems under earthquake excitation. *Journal of Structural Engineering, 129*(8), 1036–1046.

Yao, Z., Wang, W., Fang, C., & Zhang, Z. (2020). An experimental study on eccentrically braced beam-through steel frames with replaceable shear links. *Engineering Structures, 206*, 110185.

Zamani, P., Azhari, S., Hamidia, M., & Hassani, N. (2024). Crack image-based FEMA P-58-compliant fragility models for automated earthquake-induced loss estimation in non-ductile RC moment frames. *Structures, 60*, 105873.

Zamani, P., Hamidia, M., & Hassani, N. (2024). Probabilistic post-earthquake loss measurement for RC framed buildings using crack image analysis. *Measurement, 238*, 115286.

Zahrai, S. M., & Hamidia, M. J. (2010, October 15–16). Studying the rehabilitation of existing structures using compound system of cables and shape memory alloys. In *Improving the seismic performance of existing buildings and other structures* (pp. 1440–1448). American Society of Civil Engineers.

Zareian, F., Lignos, D. G., & Krawinkler, H. (2010, May 12–15). Evaluation of seismic collapse performance of steel special moment resisting frames using FEMA P695 (ATC-63) methodology. In *Structures Congress 2010* (pp. 1275–1286). American Society of Civil Engineers.

Zhang, X., Ma, X., & Zhang, S. (2023). Seismic performance of eccentrically braced precast reinforced concrete columns-steel beams frame with replaceable shear links based on plastic design. *Journal of Building Engineering, 76*, 107027.

Zhang, H., Su, M., Lian, M., Cheng, Q., Guan, B., & Gong, H. (2020). Experimental and numerical study on the seismic behavior of high-strength steel framed-tube structures with end-plate-connected replaceable shear links. *Engineering Structures, 223*, 111172.

Zhang, H., Lian, M., & Su, M. (2020). Study on the seismic performance of high-strength steel framed-tube structures with replaceable shear links. *Journal of Constructional Steel Research, 171*, 106131.

Zinati, M., Hassani, N., & Hamidia, M. (2026). Comparison of peak seismic displacement obtained from simplified analysis for lead rubber bearing (LRB) isolators with nonlinear response history analysis. *Interdisciplinary Journal of Civil Engineering, 2*(1), 1–15.